Springer

Acta Mechanica Sinica

CrossMark click for updates

• RESEARCH PAPER •

Acta Mech. Sin., Vol. 40, 524007 (2024)
https://doi.org/10.1007/s10409-024-24007-x

Adaptive feedback compensation control method for bipedal robot walking under continuous external disturbances

Zijing Li[1], Jinlin Zhang[1], Mengyue Lu[1], Wanchao Chi[2], Chong Zhang[2], Shenghao Zhang[2], Yuzhen Liu[2], and Chunbiao Gan[1*]

[1] *State Key Laboratory of Fluid Power and Mechatronic Systems, School of Mechanical Engineering, Zhejiang University, Hangzhou 310058, China;*
[2] *Tencent Robotics X, Tencent Binhai Building, Shenzhen 518054, China*

Received February 9, 2024; accepted April 20, 2024; published online July 1, 2024

In the past few decades, people have been trying to address the issue of walking instability in bipedal robots in uncertain environments. However, most control methods currently have still failed to achieve robust walking of bipedal robots under uncertain disturbances. Existing research mostly focuses on motion control methods for robots on uneven terrain and under sudden impact forces, with little consideration for the problem of continuous and intense external force disturbances in uncertain environments. In response to this issue, a disturbance-robust control method based on adaptive feedback compensation is proposed. First, based on the Lagrangian method, the dynamic model of a bipedal robot under different types of external force disturbances was established. Subsequently, through dynamic analysis, it was observed that classical control methods based on hybrid zero dynamics failed to consider the continuous and significant external force disturbances in uncertain environments. Therefore, an adaptive feedback compensation controller was designed, and an adaptive parameter adjustment optimization algorithm was proposed based on walking constraints to achieve stable walking of bipedal robots under different external force disturbances. Finally, in numerical simulation experiments, comparative analysis revealed that using only a controller based on hybrid zero dynamics was insufficient to converge the motion of a planar five-link bipedal robot subjected to periodic forces or bounded noise disturbances to a stable state. In contrast, in the adaptive feedback compensation control method, the use of an adaptive parameter adjustment optimization algorithm to generate time-varying control parameters successfully achieved stable walking of the robot under these disturbances. This indicates the effectiveness of the adaptive parameter adjustment algorithm and the robustness of the adaptive feedback compensation control method.

Bipedal robot, External disturbance, Walking stability, Adaptive feedback compensation, Anti-disturbance control

Citation: Z. Li, J. Zhang, M. Lu, W. Chi, C. Zhang, S. Zhang, Y. Liu, and C. Gan, Adaptive feedback compensation control method for bipedal robot walking under continuous external disturbances, Acta Mech. Sin. 40, 524007 (2024), https://doi.org/10.1007/s10409-024-24007-x

1. Introduction

The three key determinants of the working capability of bipedal robots are agility in motion, adaptability to the environment, and diversity in tasks. As research has progressed, experimental scenarios for bipedal robots have expanded from ideal environments to unstructured environments with uncertain disturbances. Despite decades of research leading to noticeable improvements in the walking performance of bipedal robots, prototypes that are practically applicable in daily life remain scarce. The DARPHA Challenge held in 2015 [1] highlighted that there is still significant room for improvement in the adaptability of bipedal robots to uncertain disturbances, not to mention their use in more complex applications such as emergency rescue [2], firefighting [3], and extraterrestrial exploration. Therefore, how bipedal robots can maintain stable walking under continuous or even unpredictable disturbances is a critical issue that urgently needs to be addressed in the current development of bipedal robots.

*Corresponding author. E-mail address: cb_gan@zju.edu.cn (Chunbiao Gan)
Executive Editor: Jian Xu

The dynamic characteristics of bipedal robot systems and external disturbances have a significant impact on achieving motion stability in uncertain environments. Therefore, it is necessary to further investigate reasonable modeling methods for robots under uncertain disturbances. Modeling methods based on ideal environments can be broadly categorized into two types. One type includes simplified models such as linear inverted pendulum (LIP) [4] and spring-loaded inverted pendulum (SLIP) [5]. The other type involves constructing multi-link dynamic models using Lagrangian equations or Newton-Euler equations. To our knowledge, previous dynamic models of bipedal robots have rarely incorporated various uncertainties encountered during robot walking, such as continuous strong winds, muddy roads or uneven surfaces, swaying walking platforms, or continuous pushing in malicious areas of the robot's body. In addressing external disturbances like these, without loss of generality, one can consider applying an external disturbance at the robot's center of mass or hip joints. As for external disturbances affecting other parts of the body, the virtual work principle can be used to derive the Jacobian matrix for the transformation of the coordinates of the point of action relative to the generalized coordinates vector. In the case of uncertainty, the disturbance can be assumed to take the form of bounded noise [6], with its intensity and spectral width adjustable according to the situation. This is commonly used to characterize external disturbances with limited spectral width and intensity, representing stochastic variations experienced by actual systems.

The control of motion stability in bipedal robots has been a challenging task. One approach is to achieve stability by dynamically adjusting the robot's gait in real-time. Gait adjustments can be accomplished through optimization-based real-time planning [7,8], trajectory generation methods inspired by lower limb movement mechanisms, such as phase-variable mapping [9] or motion-lagged coordination mapping [10], heterogeneous model for gait analysis [11] or gait transitions based on a gait library [12]. In Ref. [13], stability of the center of mass motion is achieved by providing an explicit range for the desired step duration, and a nonlinear optimizer is employed to update the walking cycle. Additionally, compensating for the trajectory energy based on the capture point theory [14], quadratic programming for tracking error, or synchronization with the zero moment point (ZMP) saturation events can be used to adjust step length and walking cycle. Model predictive control methods based on online calculations [15] have also been widely applied in recent years for disturbance rejection control [16,17]. Reference [18] proposes a framework based on a simplified model and online predictive control, reacting to disturbances and anticipating offline trajectories to counteract adverse effects generated by disturbances. Optimization-based real-time planning methods have high real-time requirements and often simplify the robot to a common dynamic equilibrium system such as an inverted pendulum. However, bipedal robots are complex tree-structured systems with multiple degrees of freedom. The real-time and accurate perception of posture and center of mass state information is challenging, making it difficult to achieve dynamic stability directly through center of mass position adjustments. Therefore, dynamic stability control is more challenging for bipedal robots. Researchers at the University of Michigan utilized virtual constraints [19] and hybrid zero dynamics (HZD) to offline optimize the generation of gaits with different speeds. They then switched gaits based on the estimated state of the robot's body, enabling the robot to walk experimentally on various terrains such as sidewalks, grass, sand, waxed surfaces, and snowy areas [20]. Ge et al. [21] further designed a multi-objective gait switching function on the basis of gait library generation. They optimized this function to obtain the reference gait for the next step and achieved stable walking in a simulation environment on randomly uneven ground. However, this gait library construction method requires a significant amount of time for offline optimization, and the non-smooth transition between different gaits during online walking may lead to instability in walking.

In addition to gait-based adjustments, rapid error convergence can be achieved by designing appropriate controllers [22]. Control methods based on HZD [23] have been successful in the underactuated walking control of bipedal robots. To obtain a stable zero dynamics manifold, the controller is typically designed to be feedback linearized with respect to lateral dynamics [24]. Building upon this, a Lyapunov function [25] can be established to construct a rapidly exponentially converging hybrid periodic orbit. Recently, Ma et al. [26] designed a low-level neural control with cubic order evolution rule by Lyapunov's stability theory, and achieved application effectiveness for better control accuracy, faster convergence speed, and lower controlled torque for a novel gait planning strategy of lower limb prosthesis; Reher and Ames [27] proposed a model-based control Lyapunov function quadratic programming controller, achieving stability of bipedal robots on uneven outdoor terrain and under external force. Nevertheless, this gain scheduling approach requires extensive and tedious parameter tuning both in simulation and real-world environments. Even with successful adjustment of a set of gains, it may still lead to steady-state errors [28] and oscillations [29]. Additionally, a self-adaptive sliding mode controller was proposed in Ref. [30] to ensure that the robot's state trajectory converges to a certain boundary layer under uncertain disturbances, extending the controller to non-flat terrain conditions. However, this method is based on inverse kinematic planning trajectories and does not consider the energy efficiency of the gait.

In response to the aforementioned issues, this work proposes a disturbance-resistant control method based on adaptive feedback compensation to achieve the walking stability of bipedal robots under different external force disturbances in uncertain environments. The structure of this work is as follows: the first section elucidates the dynamic modeling method of bipedal robots under external force disturbances; the second section presents the gait planning method for bipedal robots based on virtual constraints and HZD; the third section introduces the adaptive feedback compensation control method and the algorithm for adaptive parameter adjustment for bipedal robots; the fourth section demonstrates the application of both the traditional control method based on HZD and the further proposed disturbance-resistant control method with adaptive feedback compensation to bipedal robot control under the influence of external periodic forces or bounded noise; finally, the fifth section provides conclusions.

2. Dynamic modeling of bipedal robot walking under external force disturbances

In Fig. 1(a), the bipedal robot considered here is composed of a torso, two thighs, and two shanks. Unless otherwise specified, the following parameters are assumed: the length of the torso is $L_1 = 0.4$ m, mass is $m_1 = 12.5$ kg, and the position of the center of mass relative to the hip joint is $l_1 = 0.21$ m; each thigh has a length of $L_2 = 0.19$ m, mass $m_2 = 0.7$ kg, and the position of the center of mass relative to the hip joint is $l_2 = 0.125$ m; each shank has a length of $L_2 = 0.19$ m, mass $m_2 = 0.7$ kg, and the position of the center of mass relative to the knee joint is $l_2 = 0.125$ m. For other parameters' values, a similar analysis can be performed. In addition, q_1 is the angle of the torso relative to the vertical line, q_2 and q_3 are the angles of the two thighs relative to the torso, while q_4 and q_5 are the angles of the two shanks relative to the connected thighs, respectively. This work only considers the planar dynamics of the robot shown in Fig. 1(a) and the walking control under sustained external force disturbances shown in Fig. 1(b). Although this may seem unrealistic, in many cases, the bipedal robot dynamics can be approximately decoupled into sagittal and coronal plane dynamics. This approach is often helpful for robot's dynamic analysis, controller design, and numerical simulations [31].

As shown in Fig. 1(b), it is assumed that the hip joint of the bipedal robot is subjected to a horizontal force disturbance: $\mathbf{F}_{ex} = \begin{bmatrix} F(t) & 0 \end{bmatrix}^{\mathrm{T}}$, where $F(t)$ is a periodic or bounded noisy external force disturbance. The specific form of $F(t)$ will be provided in Sect. 4.

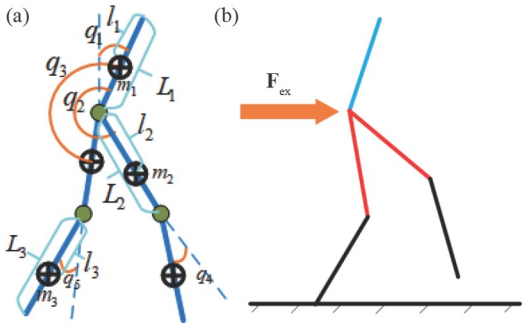

Figure 1 Schematic diagram of the link model of bipedal robot under external force disturbance. (a) Bipedal robot model; (b) external force disturbance.

In order to incorporate external force disturbances into the dynamic model of the bipedal robot, it is necessary to establish a mapping relationship between the operational space and the joint space through the Jacobian matrix:

$$\mathbf{J}(q) = \frac{\partial \mathbf{P}_c}{\partial \mathbf{q}}, \tag{1}$$

where $\mathbf{P}_c$ is the disturbance force application point position vector, and $\mathbf{q}$ is the generalized coordinate vector of the bipedal robot. Thus, the form of external force disturbance reflected in the generalized coordinates of the bipedal robot can be expressed as

$$\boldsymbol{\psi} = \mathbf{J}(q)^{\mathrm{T}}\mathbf{F}_{ex}. \tag{2}$$

During the walking process, the dynamic model of a bipedal robot can be represented by a set of differential equations describing the single support phase, along with a discrete model for the contact event when initiating dual support. Assuming $\mathcal{Q}_s$ is the configuration space of the robot during the single support phase, i.e., $\mathbf{q}_s := (q_1, q_2, q_3, q_4, q_5)^{\mathrm{T}} \in \mathcal{Q}_s$, it can serve as a set of generalized coordinates for the robot, where the subscript "s" denotes the single support phase.

During the single support phase, the dynamic equations for this phase, considering the external force disturbance described by the Lagrange equation and Eq. (2), can be expressed as follows:

$$\mathbf{D}_s(\mathbf{q}_s)\ddot{\mathbf{q}}_s + \mathbf{C}_s(\mathbf{q}_s, \dot{\mathbf{q}}_s)\dot{\mathbf{q}}_s + \mathbf{G}_s(\mathbf{q}_s) = \mathbf{B}_s(\mathbf{q}_s)\mathbf{u} + \boldsymbol{\psi}, \tag{3}$$

where $\mathbf{D}_s(\mathbf{q}_s)$ is the inertia matrix, $\mathbf{C}_s(\mathbf{q}_s, \dot{\mathbf{q}}_s)$ is the Coriolis matrix, $\mathbf{G}_s(\mathbf{q}_s)$ is the gravity vector, $\mathbf{B}_s(\mathbf{q}_s)$ is the input matrix, $\mathbf{u}$ is the control force vector, and $\boldsymbol{\psi}$ represents the external force disturbance described in Eq. (2).

Defining the state vector of the bipedal robot as $\mathbf{x} = \begin{bmatrix} q & \dot{q} \end{bmatrix}^{\mathrm{T}}$, the differential equations for the single support phase of the bipedal robot can be transformed into

$$\dot{\mathbf{x}} = \mathbf{f}(x) + \mathbf{g}(x)\mathbf{u} + \mathbf{f}_{ex}, \tag{4}$$

where

$$\mathbf{f}(\mathbf{x}) = \begin{bmatrix} \dot{\mathbf{q}}_s & -\mathbf{D}_s(\mathbf{q}_s)^{-1}\left[\mathbf{C}_s(\mathbf{q}_s, \ddot{\mathbf{q}}_s)\dot{\mathbf{q}}_s + \mathbf{G}_s(\mathbf{q}_s)\right] \end{bmatrix}^{\mathrm{T}},$$

$$\mathbf{g}(\mathbf{x}) = \begin{bmatrix} \mathbf{0} & \mathbf{D}_s(\mathbf{q}_s)^{-1}\mathbf{B}_s(\mathbf{q}_s) \end{bmatrix}^{\mathrm{T}},$$

$$\mathbf{f}_{ex} = \begin{bmatrix} \mathbf{0} & \mathbf{D}_s(\mathbf{q}_s)^{-1}\boldsymbol{\psi} \end{bmatrix}^{\mathrm{T}}.$$

When the swing leg makes contact with the ground, the robot enters the dual support phase. Assuming that the contact collision between the swing leg and the ground is instantaneous and rigid, there is no change in pose during the collision process, and the leg end does not rebound from the ground. At this point, the coordinate vector of the swing leg end position, denoted as $\mathbf{P}_{sw} = [x_{sw}, z_{sw}]^{\mathrm{T}}$, needs to be added to the generalized coordinates of the robot, i.e., $\mathbf{q}_e := (\mathbf{x}_{sw}, \mathbf{z}_{sw}, \mathbf{q}_1, \mathbf{q}_2, \mathbf{q}_3, \mathbf{q}_4, \mathbf{q}_5) \in \mathcal{Q}_e$. Also, since there is no sudden change in pose during the collision process, according to the law of conservation of angular momentum, the following collision model can be derived:

$$\mathbf{q}_e^+ = \mathbf{q}_e^-, \tag{5}$$

$$\begin{bmatrix} \mathbf{D}_e(\mathbf{q}_e^+) & -\mathbf{E}' \\ \mathbf{E} & \mathbf{0} \end{bmatrix} \begin{bmatrix} \dot{\mathbf{q}}_e^+ \\ \mathbf{f}_{ct} \end{bmatrix} = \begin{bmatrix} \mathbf{D}_e(\mathbf{q}_e^-)\dot{\mathbf{q}}_e^- \\ \mathbf{0} \end{bmatrix}, \tag{6}$$

where $\mathbf{q}_e^-$ and $\mathbf{q}_e^+$ are the generalized coordinates, and $\dot{\mathbf{q}}_e^-$ and $\dot{\mathbf{q}}_e^+$ are the generalized velocities before and after the collision, respectively. Additionally, $\mathbf{D}_e(\mathbf{q}_e^-)$ and $\mathbf{D}_e(\mathbf{q}_e^+)$ are the inertia matrices before and after the collision, $\mathbf{E}$ is the Jacobian matrix of the swing leg end position coordinates relative to the generalized coordinates, and $\mathbf{f}_{ct}$ is the ground reaction force acting on the swing leg during the collision. The collision model for the bipedal robot entering the dual support phase can be further simplified as

$$\mathbf{x}_e^+ := \Delta(\mathbf{x}_e^-). \tag{7}$$

Combining Eqs. (4) and (7), the complete dynamic model of the bipedal robot under external force disturbances is given by

$$\begin{cases} \dot{\mathbf{x}} = \mathbf{f}(\mathbf{x}) + \mathbf{g}(\mathbf{x})\mathbf{u} + \mathbf{f}_{ex}, & \mathbf{x} \notin \mathbf{S}, \\ \mathbf{x}_e^+ = \Delta(\mathbf{x}_e^-), & \mathbf{x} \in \mathbf{S}, \end{cases} \tag{8}$$

where $\mathbf{S} = \left\{\mathbf{x} \mid z_{sw}(\mathbf{x}) = 0, \dot{z}_{sw}(\mathbf{x}) < 0\right\}$ represents the switching surface. At this point, the robot collides with the ground, and the single support phase comes to an end.

3. Gait generation and analysis of external force disturbance resistance based on virtual constraints and HZD

In this section, a brief analysis is conducted on the effectiveness of the gait planning method based on virtual constraints and HZD [24] under small external force disturbance conditions. By transforming the gait parameter selection problem into a nonlinear optimization problem and designing an initial gait and controller for a bipedal robot, this sets the groundwork for the subsequent proposal of adaptive feedback compensation control methods.

3.1 Virtual constraint design

Virtual constraints are defined as a set of output functions used to regulate the desired motion of the robot [24]. The main idea is to design a feedback controller to adjust the output functions so that their output is zero, thereby achieving tracking and control of the reference trajectory.

The output function is defined as follows:

$$\mathbf{y} = \mathbf{h}(\mathbf{q}) := \mathbf{h}_0(\mathbf{q}) - \mathbf{h}_d(\theta(\mathbf{q})), \tag{9}$$

where $\mathbf{h}_0(\mathbf{q})$ is the active control term, which is a vector composed of the active degrees of freedom of the bipedal robot:

$$\mathbf{h}_0(\mathbf{q}) = (q_2 \quad q_3 \quad q_4 \quad q_5)^{\mathrm{T}}. \tag{10}$$

Meanwhile, $\theta(\mathbf{q})$ is an underactuated variable that strictly monotonically increases or decreases during the walking process of the bipedal robot. In this context, this work defines $\theta(\mathbf{q})$ as the absolute angle between the supporting foot and the line connecting the hips. $\mathbf{h}_d(\theta(\mathbf{q}))$ represents the desired evolution trajectory of the active degrees of freedom, designed in the form of a sixth-order Bézier polynomial as follows:

$$\mathbf{h}_d(\theta(\mathbf{q})) = \mathbf{b}_v(\tau) = \sum_{k=0}^{6} \boldsymbol{\alpha}_k \frac{6!}{k!(6-k)!}\tau^k(1-\tau)^{6-k}, \tag{11}$$

where the real parameter vector $\boldsymbol{\alpha}_k$ (k = 0, 1, …, 6) represents the coefficients of the virtual constraint that need to be optimized, τ is the normalized independent variable: $\tau = (\theta - \theta_{ini})/(\theta_f - \theta_{ini})$, while θ_{ini} and θ_f are the initial and final values of θ, respectively.

3.2 Controller design based on HZD

Taking the second derivative of the output function with respect to the control input, the relationship between the control torque and the output function can be expressed as follows:

$$\ddot{\mathbf{y}} = \left[\frac{\partial}{\partial \mathbf{q}}\left(\frac{\partial \mathbf{y}}{\partial \mathbf{q}}\dot{\mathbf{q}}\right)\frac{\partial \mathbf{y}}{\partial \mathbf{q}}\right]\mathbf{f}(\mathbf{x}) + \frac{\partial \mathbf{y}}{\partial \mathbf{q}}\mathbf{g}(\mathbf{x})\mathbf{u}. \tag{12}$$

Therefore, the controller can be designed as

$$\mathbf{u} = (L_g L_f \mathbf{y})^{-1}(-L_f^2 \mathbf{y} + \mathbf{v}), \tag{13}$$

$$\mathbf{v} = \ddot{\mathbf{y}}, \tag{14}$$

where L_f and L_g are the *Lie* derivatives with respect to $\mathbf{f}(\mathbf{x})$ and $\mathbf{g}(\mathbf{x})$, respectively [21]. By applying the HZD approach [16], $\mathbf{v}$ can be expressed as

$$\mathbf{v} = -\frac{K_p}{\varepsilon^2}\mathbf{y} - \frac{K_d}{\varepsilon}\dot{\mathbf{y}}. \tag{15}$$

Thus, the trajectory of the bipedal robot can converge to the zero dynamics manifold: $\mathbf{Z}_v = \{\mathbf{x}_v \mid \mathbf{y}_v = \mathbf{0}, \dot{\mathbf{y}}_v = \mathbf{0}\}$, where the parameters $K_p > 0$, $K_d > 0$, and $\varepsilon > 0$. In this way, the controller can be rewritten as

$$\mathbf{u}_{HZD} = -(L_g L_f \mathbf{y})^{-1}\left(L_f^2\mathbf{y} + \frac{K_p}{\varepsilon^2}\mathbf{y} + \frac{K_d}{\varepsilon}\dot{\mathbf{y}}\right). \tag{16}$$

By appropriately adjusting the parameters K_p, K_d and ε, the output function of the bipedal robot can converge to the aforementioned zero dynamics manifold within a finite time.

3.3 Gait generation and analysis of resistance to external force disturbances

Based on the virtual constraints and controller design mentioned above, the following assumptions are made regarding the bipedal robot's walking, stability, and output function:

(1) Single support and double support phases alternate, and the double support phase is simplified as an instantaneous rigid collision process.

(2) After a collision, the swing foot velocity drops to zero, with no slipping or rebound. The joint angles of the robot do not change before and after the collision, but joint velocities experience a jump.

(3) Due to frictional forces, the yaw degree of freedom remains stationary throughout the entire single support phase.

(4) After the collision phase, there is a coordinate swap between the swing leg and the support leg.

(5) There is at least one fixed point, and this fixed point is asymptotically stable.

(6) The output function satisfies the characteristics of HZD.

Furthermore, by minimizing the following objective function concerning the energy of the bipedal robot:

$$J(\boldsymbol{\alpha}) := \int_0^T \| \mathbf{u}_{HZD} \|_2^2 \, \mathrm{d}t, \tag{17}$$

where T is the set walking period. By taking the virtual constraint parameter vector $\boldsymbol{\alpha}_k$ (k = 0, 1, …, 6) from the fitted Bézier curve in Eq. (11) as optimization variables and utilizing the FMINCON function in MATLAB for solving, a periodic gait for the bipedal robot can be generated. The robot's center of mass trajectory for the first 2 s of this periodic gait obtained through this method is illustrated in Fig. 2(a)-(c).

To analyze the impact of different disturbances on the walking dynamics of the bipedal robot, constant force disturbance ($F \equiv 7$ N), harmonic force disturbance ($F = 10\sin(2\pi t)$ N), and impulsive force disturbance ($F = 15$ N) are applied to the robot based on variations in the duration and intensity of equivalent force disturbances. The disturbance times are set to be after 2 s of walking. The simulation results are shown in Fig. 2. It should be noted that as the amplitude of external force disturbance continues to increase, the bipedal robot will become unstable and fall.

From Fig. 2, it can be observed that when constant or harmonic external forces act on the hip joints of the bipedal robot, the controller based on HZD can transition the robot from one stable gait to another over a single gait cycle. In the case of equivalent impulsive force disturbances, the controller can stabilize the gait back to the original periodic gait. Therefore, for small external force disturbances, the HZD-based controller is effective. Despite the differences in control outcomes after constant or harmonic force disturbances compared to the original gait, the robot can continue walking without falling.

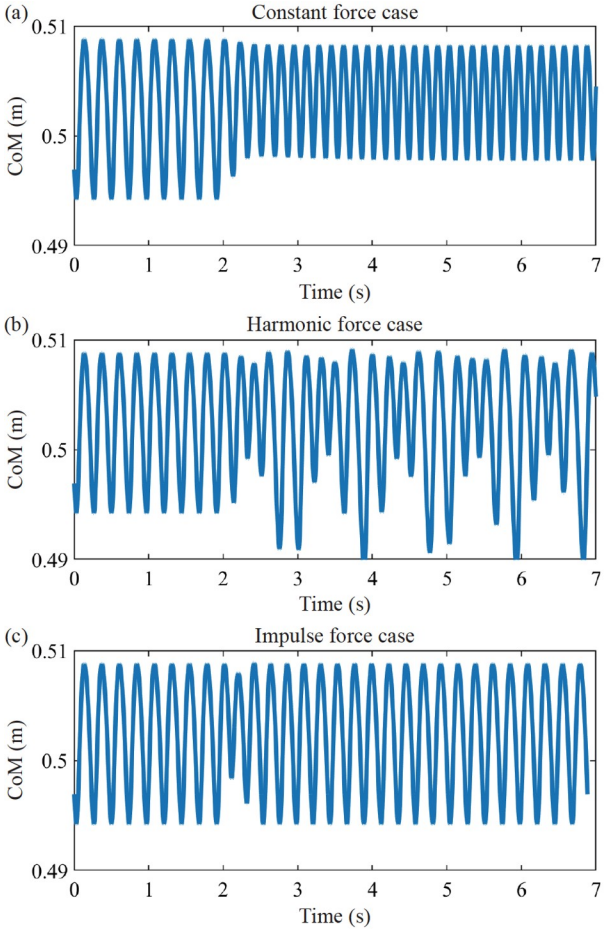

Figure 2 CoM trajectories of bipedal robot under various external force disturbances.

4. Adaptive feedback compensation control method

The controller designed based on the HZD, as shown in Eq. (17), can typically achieve asymptotically stable walking of the bipedal robot under small disturbances. However, when external disturbance intensity is significant, if the controller cannot promptly adjust to the errors, it may lead to the instability of the robot's walking, ultimately resulting in a fall, as seen in the relevant simulation results in Sect. 4. To enhance the robustness of walking control for the robot, an adaptive feedback compensation control method is proposed. This method involves adding a feedback compensation adjustment component to the original controller. By adaptively adjusting the control parameters based on feedback from the robot's walking state, it aims to achieve stable walking of the robot under continuously changing external disturbances, preventing falls.

4.1 Feedback compensation adjustment

Firstly, after the completion of each full walking cycle of the robot, a compensation adjustment is considered for the controller parameters K_p and K_d based on the feedback from the walking state:

$$K_\mathrm{p}^{(i)} = K_\mathrm{p}^{\mathrm{HZD}} + \xi_i, \tag{18}$$

$$K_\mathrm{d}^{(i)} = K_\mathrm{d}^{\mathrm{HZD}} + \zeta_i, \tag{19}$$

where $K_\mathrm{p}^{(i)}$ and $K_\mathrm{d}^{(i)}$ are the values of K_p and K_d at the i-th step, $K_\mathrm{p}^{\mathrm{HZD}}$ and $K_\mathrm{d}^{\mathrm{HZD}}$ are the original values of K_p and K_d in the HZD controller, and ξ_i and ζ_i are the compensation adjustment values for K_p and K_d at step i. This way, the controller at step i can be adjusted as follows:

$$\mathbf{u}_i = -L_\mathrm{g}L_\mathrm{f}\mathbf{y}^{-1}\left(L_\mathrm{f}^2\mathbf{y} + \frac{K_\mathrm{p}^{(i)}}{\varepsilon^2}\mathbf{y} + \frac{K_\mathrm{d}^{(i)}}{\varepsilon}\dot{\mathbf{y}}\right). \tag{20}$$

Next, substituting Eqs. (18) and (19) into Eq. (20) yields

$$\mathbf{u}_i = \mathbf{u}_{\mathrm{HZD}} + \mathbf{u}_{\mathbf{AB},i}, \tag{21}$$

where

$$\mathbf{u}_{\mathbf{AB},i} = \mathbf{A}_i\mathbf{y} + \mathbf{B}_i\dot{\mathbf{y}},$$

$$\mathbf{A}_i = -L_\mathrm{g}L_\mathrm{f}\mathbf{y}^{-1}\frac{\xi_i}{\varepsilon^2},$$

$$\mathbf{B}_i = -L_\mathrm{g}L_\mathrm{y}\mathbf{y}^{-1}\frac{\zeta_i}{\varepsilon}.$$

From Eq. (21), it can be seen that the controller at step i consists of the original HZD-based controller and a feedback compensator based on the parameter matrices $\mathbf{A}_i$ and $\mathbf{B}_i$.

Finally, during the walking process, the update of parameters K_p and K_d for the bipedal robot after each step is transformed into an adjustment of the parameter matrices $\mathbf{A}_i$ and $\mathbf{B}_i$ based on its walking state. Since the goal of the controller is to make the robot's trajectory converge to the zero dynamics manifold, and the form of $\mathbf{u}_{\mathbf{AB},i}$ is similar to that of a PD controller, the adjustment of the parameter matrices $\mathbf{A}_i$ and $\mathbf{B}_i$ can be directly based on a PD controller tuning strategy:

$$\mathbf{A}_i = a_i\mathbf{I}, \tag{22}$$

$$\mathbf{B}_i = b_i\mathbf{I}, \tag{23}$$

where a_i and b_i are the changes in the parameter matrices $\mathbf{A}_i$ and $\mathbf{B}_i$ at step i, $\mathbf{I}$ is the identity matrix, and the relationship between a_i and b_i must take the following form:

$$4a_i = b_i^2 \tag{24}$$

to obtain a critically damped closed-loop performance, i.e., the damping coefficient is set to twice the square root of the stiffness in the PD controller $\mathbf{u}_{\mathbf{AB},i}$ [32].

Based on the above analysis, the control block diagram for bipedal robot walking using the proposed adaptive feedback compensation method is illustrated in Fig. 3.

4.2 Parameter adaptive adjustment algorithm

When external force disturbances continuously change, maintaining the adjustment values a_i and b_i the same as the previous step can lead to an increase in the error between the expected and actual walking gaits. This may result in various issues for the bipedal robot during walking, such as sliding of the supporting leg, inconsistent forces between the swing leg and the ground during collisions, knee joint buckling, and even falls. Therefore, it is necessary to assess these situations in real-time during the robot's walking process and dynamically adjust the parameter matrices ac-

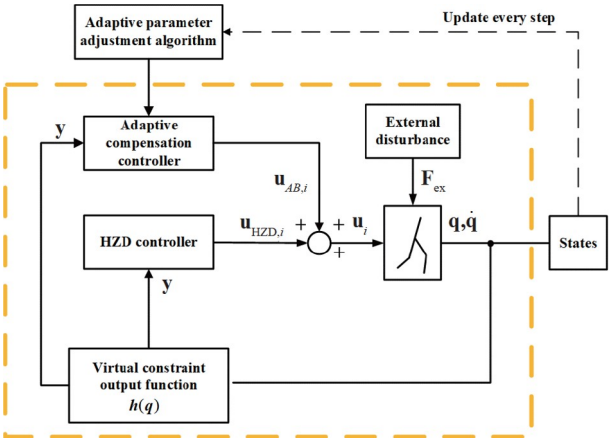

Figure 3 Block diagram of adaptive feedback compensation control of bipedal walking.

cordingly. The flowchart is shown in Fig. 4. The steps of the parameter adaptive adjustment algorithm are briefly summarized as follows:

Step 1: Set the initial state of the bipedal robot, x_0, determine the maximum number of walking steps N, and initialize the adjustment values for the parameters $a_0 = 0$ and $b_0 = 0$.

Step 2: Integrate the state matrix of the bipedal robot within one step using Eqs. (8) and (21).

Step 3: Calculate the position of the swing leg P_{sw} using the kinematics of the bipedal robot:

$$\begin{aligned} P_{sw} = {} & L_2 \times \sin(q_2 + q_1) + L_3 \times \sin(q_2 + q_4 + q_1) \\ & - L_2 \times \sin(q_3 + q_1) - L_3 \times \sin(q_3 + q_5 + q_1), \end{aligned} \tag{25}$$

and based on the position of the swing leg, determine whether to take a step forward. If the swing leg has completed a full step forward, proceed to the next step. Otherwise, consider the current state as the initial state x_0 for the next integration calculation and return to Step 2 for further integration.

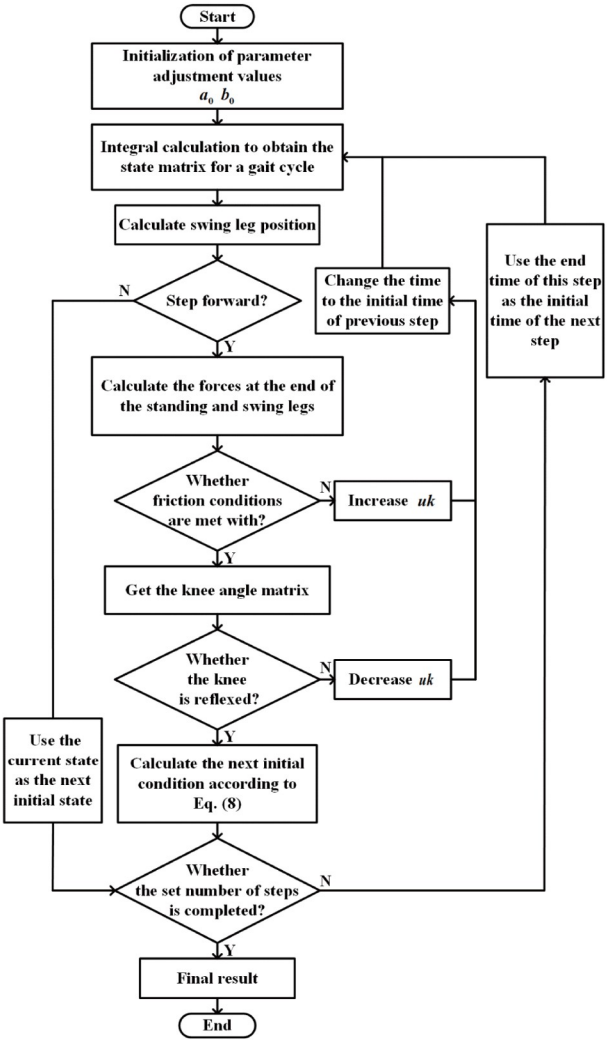

Figure 4 Flowchart of parameter adaptive adjustment algorithm.

Step 4: Calculate the force $\mathbf{F}_{st}$ on the supporting leg throughout the process using Eq. (3). Analyze the force $\mathbf{F}_{sw}$ on the swing leg during collisions based on Eq. (8). Determine if the frictional forces meet the friction conditions based on the preset friction coefficient [26]. If they do, proceed to the next step; otherwise, adjust the parameters a_i and b_i in Eqs. (22) and (23). The specific form is as follows:

$$a_i = uk_i^2, \tag{26}$$

$$b_i = 2 \times uk_i, \tag{27}$$

$$uk_i = uk_{i-1} + \Delta k_1, \tag{28}$$

where Δk_1 is an increment for step length adjustment, and in this context, it is set to 0.5. Then, reset the time to the initial time of this step and return to Step 2 for integration.

Step 5: Obtain the knee joint angle based on the state matrix of the bipedal robot from Step 2. Then, determine if there is a buckling situation at the knee joint. If there is no buckling, proceed to the next step; otherwise, adjust Eq. (28).

$$uk_i = uk_{i-1} - \Delta k_2, \tag{29}$$

where Δk_2 is a decrement for step length adjustment, and in this context, it is set to 0.2. Then, reset the time to the initial time of the current step and return to Step 2 for integration.

Step 6: Calculate the initial condition x_0 for the next step using Eq. (8).

Step 7: Determine whether the maximum number of walking steps N has been reached. If not, set the current step end time as the initial time for the next step and return to Step 2 for integration. Otherwise, output the characteristic results for each step, and the algorithm terminates.

5. Simulation validation

In this section, we present failure cases of the bipedal robot's controller based on HZD under four types of deterministic and uncertain large external force disturbances. It is important to note that this section no longer considers pulse and constant external force disturbance scenarios. Instead, the focus is on continuous disturbances with varying amplitudes and frequencies (such as bounded noise) to analyze the different effects of excitation frequency and intensity on the bipedal robot's walking dynamics. Other types of external force disturbance scenarios can be similarly analyzed. Subsequently, adaptive adjustment is made to the parameter uk, and the control outcomes under these four types of large disturbances are discussed and analyzed. This aims to validate the robustness of the proposed adaptive feedback compensation control method.

Different types of periodic excitations and bounded noise excitations are shown in Fig. 5. In all periodic excitations,

the circular frequency is 2π. The amplitudes for sinusoidal and sawtooth wave excitations are 30 N, while the amplitude for square wave excitation is 22.5 N. Additionally, the expression for bounded noise excitation is

$$\eta(t) = A\cos[\Omega t + \sigma W(t) + \gamma], \tag{30}$$

where A is the intensity of the bounded noise excitation (set to 30 N), Ω is the center frequency, σ is the spectral width parameter, $W(t)$ is the unit Wiener process, and γ is a random phase uniformly distributed over $[0, 2\pi)$ [6]. The expression for the double-sided power spectral density of $\eta(t)$ is

$$S_\eta(\omega) = \frac{1}{2\pi}\left[\frac{\sigma^2}{4(\omega-\Omega)^2+\sigma^4} + \frac{\sigma^2}{4(\omega+\Omega)^2+\sigma^4}\right]. \tag{31}$$

From Eq. (31), it can be observed that by adjusting the value of the spectral width parameter σ, bounded noise can be used to simulate narrowband or wideband random processes. This is commonly employed to characterize turbulent flow in the wind, ground motion during earthquakes, and amplitude or band-limited random excitations on particle or rigid body systems. An illustrative sample of bounded noise excitation obtained through the Monte Carlo method is shown in Fig. 5(d), in which $\Omega = 1$, $\sigma = 1$.

Figure 6 shows the center of mass trajectory of the bipedal robot under the large external force disturbances using only the HZD-based controller. From Fig. 6, it can be observed that for any type of disturbance, the position of the robot's center of mass rapidly descends to zero after several normal walking steps, indicating a fall. This suggests that the HZD-based control method alone is insufficient to handle continuously changing and large-amplitude disturbances. Interestingly, in the case of bounded noise excitation, the robot can walk for more than 2 s without falling. This can be explained by the relatively small intensity of the excitation during the first 2 s (see Fig. 5(d)), indicating that the HZD-based control method is still effective. However, when the excitation intensity exceeds 20 N, the robot quickly falls. Therefore, the following conclusion can be drawn: In comparison to the form or frequency of excitation, the intensity of external force disturbances has a greater impact on the walking dynamics of the bipedal robot. It is necessary to dynamically adjust the controller gains in real-time during the control process to reduce the error between the desired trajectory and the actual walking trajectory, thus enhancing the robustness of walking control for the robot.

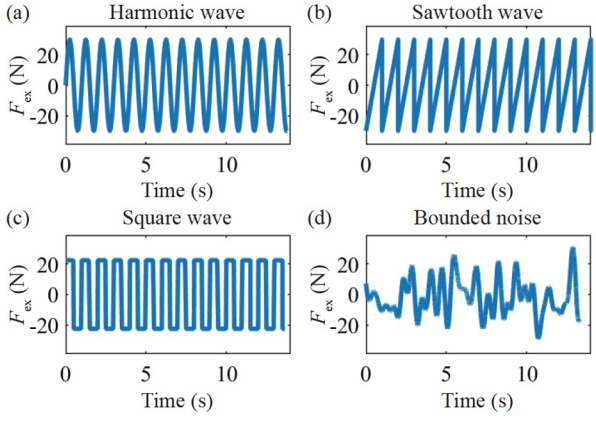

Figure 5 Four kinds of external force disturbances.

From Fig. 6(a)-(c), it can be observed that the bipedal robot quickly loses stability and the center of mass height rapidly drops to zero when subjected to harmonic or square wave excitation. Therefore, the adaptive feedback compensation control method proposed in this study quickly takes effect, as seen in the variation curves of the control parameter *uk* shown in Fig. 7(a)-(c). These curves are obtained from the parameter adaptive adjustment algorithm presented in Sect. 3.2, which updates the parameter matrices $\mathbf{A}_i$ and $\mathbf{B}_i$ at each step to cope with continuously changing external force disturbances. On the other hand, for the cases of sawtooth wave or bounded noise excitation, the center of mass position of the bipedal robot is effectively controlled by the HZD-based controller in the first 1 or 2 s (see Fig. 7 (b), (d)). Therefore, the control parameter *uk* remains zero during these time intervals, and there is no need for adaptive feedback compensation. Subsequently, the adaptive feedback compensation process is initiated due to the failure of the controller.

Additionally, from Fig. 7, it can be observed that the variation of the control parameter *uk* is not continuous. When the error between the desired trajectory and the actual walking trajectory accumulates to a certain extent, the value of *uk* will experience a jump (corresponding to the peak value of the center of mass height of the bipedal robot as shown in Fig. 8). This is done to achieve balance control for the robot's walking.

In general, the gait of a bipedal robot controlled by the HZD-based controller appears periodic, as shown in Fig. 2 in the previous Sect. 2. This is a result of the asymptotically

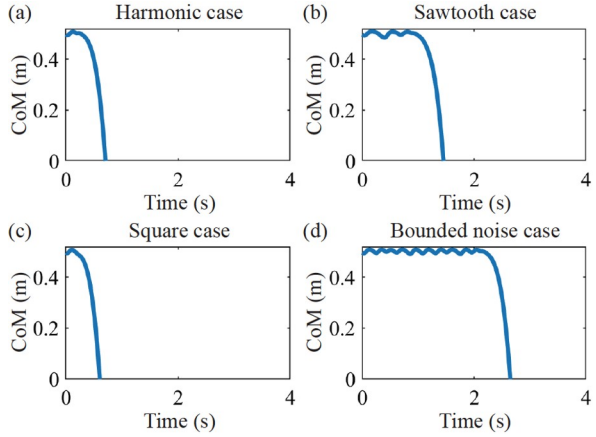

Figure 6 CoM trajectories of bipedal robot with controller based on HZD.

stable gait achieved through the integration of virtual constraint design, HZD method, and optimization algorithms. When the bipedal robot is subjected to periodic external force disturbances, even with the addition of adaptive feedback compensation to the controller, allowing real-time adjustments of the corresponding control parameters, the controlled robot's gait or center of mass position still exhibits a certain degree of periodicity, as can be seen from the results in Fig. 8(a)-(c). This is evident despite the fact that the variations in the corresponding control parameters may not necessarily reflect periodicity (see Fig. 7).

When a bipedal robot walks in an uncertain environment, the real-time adjustment of control parameters allows for changes in the robot's gait, such as step length, period, and walking direction, enabling it to maintain walking balance under bounded noise excitation. Although the gait or center of mass height variation curve may appear non-periodic, as shown in Fig. 8(d), the robot can continue walking without falling. Clearly, Fig. 8(d) demonstrates variations in step length and the duration of each step, illustrating the robustness of the adaptive feedback compensation controller to random disturbances. It is important to note that the results presented here pertain to walking in a planar scenario, and the directional aspects of walking are not addressed. Additionally, it should be emphasized that as the amplitude of the four forms of external force disturbances continues to increase, the bipedal robot will lose stability and fall. Nevertheless, the proposed adaptive feedback compensation

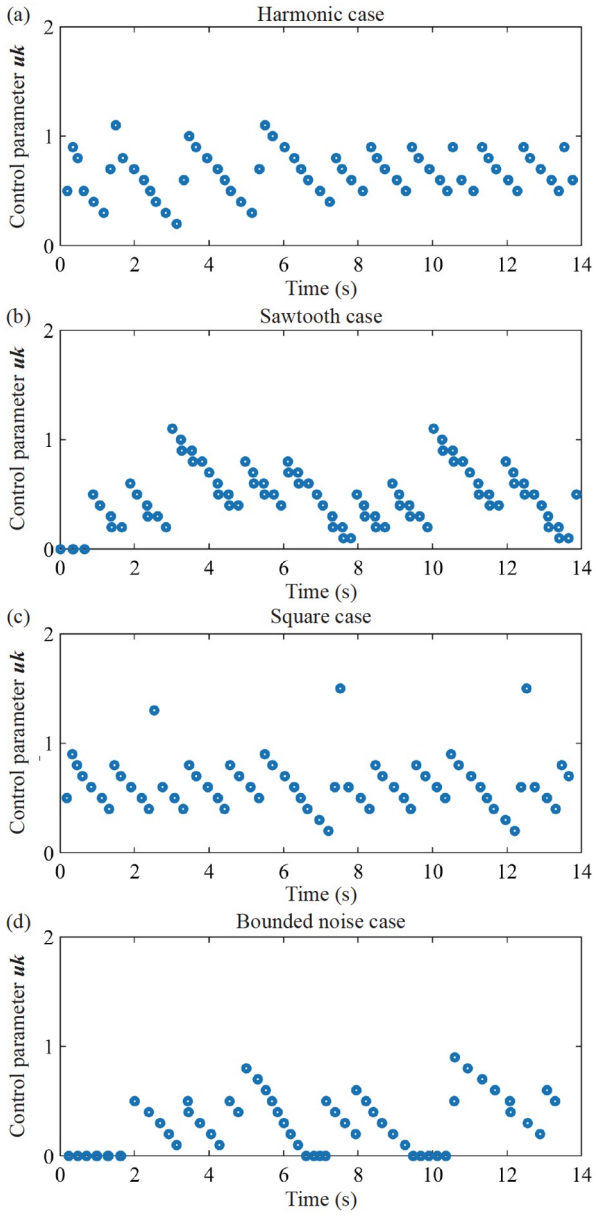

Figure 7 Control parameter *uk* generated by the parameters' adaptative adjustment algorithm.

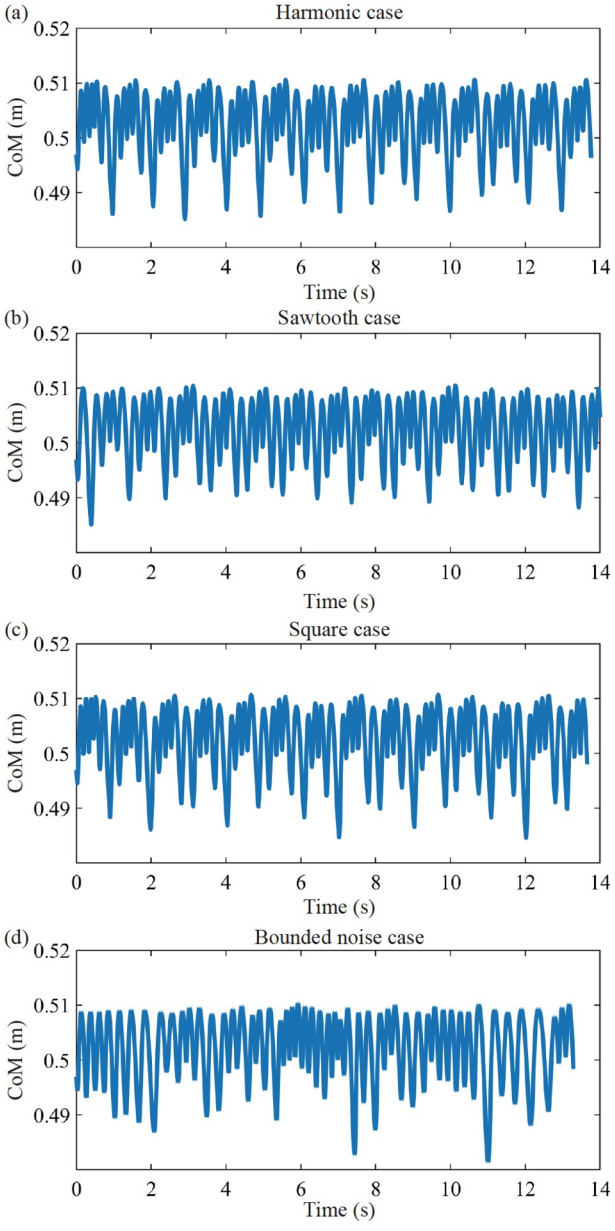

Figure 8 CoM trajectories of bipedal robot under adaptive feedback compensation control.

control method significantly enhances the robot's disturbance rejection capability. Compared to traditional controllers based solely on HZD, the robot can resist disturbances with nearly twice the amplitude.

6. Conclusion

This study investigated the adaptive control problem of dynamically walking bipedal robots under external force disturbances. An analysis and characterization of external disturbances were conducted, and the equivalent forces were mapped to the joint space of the robot through the Jacobian matrix. Based on assumptions about the gait and collisions of bipedal robots, the hybrid dynamics model of the bipedal robot under external force disturbances was established using the Lagrangian method. Simulation results indicate that the classical HZD-based controller is effective in resisting small external force disturbances. However, it fails in cases of large external force disturbances, leading to instability and even falling of the bipedal robot.

Therefore, this study proposes an adaptive feedback compensation control method. Building upon the classical HZD-based controller design, an algorithm for adaptive adjustment of parameters based on the walking state was developed. This algorithm considers factors such as the friction conditions of the bipedal robot during walking, knee joint angles, and center of mass position to analyze walking instability. It generates suitable control parameters under continuous external force disturbances. By dynamically adjusting the control parameters online, adaptive feedback control of the state output of the bipedal robot was achieved. This allows the bipedal robot to maintain balanced walking under various equivalent force disturbances with amplitudes up to one-fifth of the robot's weight. The results of the proposed adaptive feedback compensation control demonstrate that, in comparison to the form or frequency of excitation, the intensity of external force disturbances has a greater impact on the walking dynamics of the bipedal robot. Real-time adjustment of controller gains is necessary during the control process to reduce the error between the desired trajectory and the actual walking trajectory, thereby improving the robustness of walking control for the robot. Additionally, real-time adjustment of control parameters can be used to change the gait step length, period, or walking direction of the bipedal robot.

Conflict of interest *On behalf of all authors, the corresponding author states that there is no conflict of interest.*

Author contributions ***Zijing Li:*** *Development of methodology; creation of models; conducting the research and investigation process, specifically performing the data collection; preparation, creation and presentation of the published work, specifically visualization/data presentation; original draft, including preparation and creation of the published work.* ***Jinlin Zhang:*** *Design of methodology; application of mathematical and computational techniques to analyze study data.* ***Mengyue Lu:*** *Development of methodology; application of mathematical and computational techniques to analyze study data.* ***Wanchao Chi:*** *Oversight for the research activity planning; provision of study materials, laboratory samples and computing resources; partially financial support for the project leading to this publication.* ***Chong Zhang:*** *Oversight for the research activity planning; provision of study materials, laboratory samples and computing resources; partially financial support for the project leading to this publication.* ***Shenghao Zhang:*** *Oversight for the research activity planning; provision of study materials, laboratory samples and computing resources; partially financial support for the project leading to this publication.* ***Yuzhen Liu:*** *Oversight for the research activity planning; provision of study materials, laboratory samples and computing resources; partially financial support for the project leading to this publication.* ***Chunbiao Gan:*** *Oversight and leadership responsibility for the research activity planning and execution, including mentorship external to the core team; conceptualization – ideas, formulation and evolution of overarching research goals and aims; review & editing – preparation, creation and presentation of the published work.*

Acknowledgements *This work was supported by the National Natural Science Foundation of China (Grant No. 12332003), CIE-Tencent Robotics X Rhino-Bird Focused Research Program, and Zhejiang Provincial Natural Science Foundation of China (Grant No. LY23E050010).*

1 M. Spenko, S. Buerger, K. Iagnemma, and D. Shane, The DARPA Robotics Challenge Finals: Humanoid Robots To The Rescue (Springer, Cham, 2018).
2 Y. Gao, Y. Gong, V. Paredes, A. Hereid, and Y. Gu, in Time-Varying ALIP model and robust foot-placement control for underactuated bipedal robot walking on a swaying rigid surface: Proceedings of American Control Conference (ACC), San Diego, 2023.
3 B. Harish, and R. Puviarasi, Design of biped locomotive system for firefighting robot capable of human detection, Indian J. Public Health Res. & Develop. **8**, 1196 (2017).
4 S. Kajita, and K. Tani, Study of dynamic walk control of a biped robot on rugged terrain, T. SICE **27**, 177 (1991).
5 R. Blickhan, The spring-mass model for running and hopping, J. Biomech. **22**, 1217 (1989).
6 Y. K. Lin, and G. Q. Cai, Probabilistic Structural Dynamics-Advanced Theory and Applications (McGraw-Hill, Singapore, 1995).
7 A. K. Kashyap, A. Pandey, A. Chhotray, and D. R. Parhi, Controlled gait planning of humanoid robot NAO based on 3D-LIPM model, SSRN Electron. J. 2020.
8 X. Xiong, and A. Ames, 3-D underactuated bipedal walking via H-LIP based gait synthesis and stepping stabilization, IEEE Trans. Robot. **38**, 2405 (2022).
9 D. Quintero, D. J. Villarreal, D. J. Lambert, S. Kapp, and R. D. Gregg, Continuous-phase control of a powered knee-ankle prosthesis: Amputee experiments across speeds and inclines, IEEE Trans. Robot. **34**, 686 (2018).
10 Y. Lv, J. Xu, H. Fang, X. Zhang, and Q. Wang, Data-mined continuous hip-knee coordination mapping with motion lag for lower-limb prosthesis control, IEEE Trans. Neural Syst. Rehabil. Eng. **30**, 1557 (2022).
11 Y. Lv, H. Fang, J. Xu, and X. X. Zhang, in A heterogeneous model for gait analysis of the lower-limb and the prosthesis coupled system: Proceedings of ASME International Design Engineering Technical Conferences and Computers and Information in Engineering Conference, St. Louis, 2020.
12 F. Liao, Y. Zhou, and Q. Zhang, Gait transition and orbital stability analysis for a biped robot based on the V-DSLIP model with torso and swing leg dynamics, Nonlinear Dyn. **108**, 3053 (2022).
13 T. Yamamoto, and T. Sugihara, Foot-guided control of a biped robot through ZMP manipulation, Adv. Robot. **34**, 1472 (2020).
14 J. Pratt, J. Carff, S. Drakunov, and A. Goswami, in Capture point: A

step toward humanoid push recovery: Proceedings of 6th IEEE-RAS International Conference on Humanoid Robots, Genova, 2006.
15 M. Bjelonic, R. Grandia, M. Geilinger, O. Harley, V. S. Medeiros, V. Pajovic, E. Jelavic, S. Coros, and M. Hutter, Offline motion libraries and online MPC for advanced mobility skills, Int. J. Robot. Res. **41**, 903 (2022).
16 Y. Sun, W. L. Ubellacker, W. L. Ma, X. Zhang, C. Wang, N. V. Csomay-Shanklin, M. Tomizuka, K. Sreenath, and A. D. Ames, Online learning of unknown dynamics for model-based controllers in legged locomotion, IEEE Robot. Autom. Lett. **6**, 8442 (2021).
17 J. Arcos-Legarda, J. Cortes-Romero, A. Beltran-Pulido, and A. Tovar, Hybrid disturbance rejection control of dynamic bipedal robots, Multibody Syst. Dyn. **46**, 281 (2019).
18 G. Gibson, O. Dosunmu-Ogunbi, Y. Gong, and J. Grizzle, Terrain-aware foot placement for bipedal locomotion combining model predictive control, virtual constraints, and the ALIP, arXiv: 2109.14862v1.
19 K. Akbari Hamed, and J. W. Grizzle, Reduced-order framework for exponential stabilization of periodic orbits on parameterized hybrid zero dynamics manifolds: Application to bipedal locomotion, Nonlinear Anal.-Hybrid Syst. **25**, 227 (2017).
20 Y. K. Gong, R. Hartley, X. Y. Da, A. Hereid, O. Harib, J. K. Huang, and J. Grizzle, in Feedback control of a Cassie bipedal robot: Walking, standing, and riding a segway: Proceedings of American Control Conference (ACC), Philadelphia, 2019.
21 Y. Ge, H. Yuan, and C. Gan, Control method of an underactuated bipedal robot based on gait transition (in Chinese), Chin. J. Theor. Appl. Mech. **50**, 871 (2018).
22 K. Rincon, I. Chairez, and W. Yu, Finite-time output feedback robust controller based on tangent barrier Lyapunov function for restricted state space for biped robot, IEEE Trans. Syst. Man Cybern Syst. **52**, 5042 (2022).
23 J. W. Grizzle, C. Chevallereau, R. W. Sinnet, and A. D. Ames, Models, feedback control, and open problems of 3D bipedal robotic walking, Automatica **50**, 1955 (2014).
24 Y. Gu, Y. Gao, B. Yao, and C. S. G. Lee, Global-position tracking control for three-dimensional bipedal robots via virtual constraint design and multiple Lyapunov analysis, J. Dynamic Syst. Measurement Control **144**, 111001 (2022).
25 A. D. Ames, K. Galloway, K. Sreenath, and J. W. Grizzle, Rapidly exponentially stabilizing control Lyapunov functions and hybrid zero dynamics, IEEE Trans. Automat. Contr. **59**, 876 (2014).
26 X. Ma, J. Xu, H. Fang, Y. Lv, and X. Zhang, Adaptive neural control for gait coordination of a lower limb prosthesis, Int. J. Mech. Sci. **215**, 106942 (2022).
27 J. Reher, and A. D. Ames, Control Lyapunov functions for compliant hybrid zero dynamic walking, arXiv: 2107.04241.
28 S. G. Tzafestas, T. E. Krikochoritis, and C. S. Tzafestas, Robust sliding-mode control of nine-link bipedal robot walking, J. Intell. Robot. Syst. **20**, 375 (1997).
29 K. Rincon-Martinez, I. Chairez, and W. Y. Liu, Mathematical modeling and robust control of a restricted state suspended biped robot implementing linear actuators for articulation mobilization, Appl. Sci. **12**, 8831 (2022).
30 H. Yuan, Y. Ge, and C. Gan, Adaptive robust control of dynamic bipedal walking under uncertain disturbances (in Chinese), J. Zhejiang Univ. (Engineering Science), **53**, 2049 (2019).
31 E. R. Westervelt, J. W. Grizzle, C. Chevallereau, J. H. Choi, and B. Morris, Feedback Control of Dynamic Bipedal Robot Locomotion (CRC press, Boca Raton, 2018).
32 M. Raibert, S. Tzafestas, and C. Tzafestas, Comparative simulation study of three control techniques applied to a bipedal robot: Proceedings of IEEE Systems Man and Cybernetics Conference-SMC, Le Touquet, 1993, pp. 494-502.

持续外力扰动下双足机器人行走的自适应反馈补偿控制方法

李子静, 张金霖, 卢梦月, 迟万超, 张冲, 张晟浩, 刘宇真, 甘春标

摘要 在过去的几十年里, 人们一直试图解决双足机器人在不确定环境中行走不稳定的问题. 然而, 目前大多数控制方法仍然无法实现双足机器人在不确定扰动下的鲁棒行走. 现有研究大多集中于不平坦地形和脉冲力下该类机器人的运动控制方法上, 很少考虑不确定环境中的连续变化且强度较大的外部力扰动问题. 针对此问题, 提出了一种基于自适应反馈补偿的扰动鲁棒控制方法. 首先, 基于拉格朗日方法, 建立了双足机器人在不同类型外力扰动下的动力学模型. 随后, 通过动力学分析发现, 基于混合零动力学的经典控制方法未能考虑不确定环境中连续变化且幅值较大的外力扰动影响. 为此, 设计了一种自适应反馈补偿控制器, 并基于步行约束条件提出了自适应参数调整优化算法, 以实现在不同外力扰动下双足机器人的稳定行走. 最后, 在数值仿真实验中通过比较分析发现, 仅采用基于混杂零动态的控制器, 无法使受周期力或有界噪声扰动作用的平面五连杆双足机器人的运动收敛到稳定状态, 而在自适应反馈补偿控制方法中通过采用自适应参数调整优化算法生成随时间变化的控制参数, 成功实现了机器人在这些扰动作用下的稳定行走, 从而表明了自适应参数调整算法的有效性和自适应反馈补偿控制方法的鲁棒性.